Journal of Organometallic Chemistry 693 (2008) 2624–2630

Contents lists available at ScienceDirect

Journal of Organometallic Chemistry

journal homepage: www.elsevier.com/locate/jorganchem

Syntheses and characterization of ferrocenylthiocarboxylate-containing coordination compounds for nonlinear optics

Haiyan Yang [a], Linke Li [a], Yinglin Song [b], Hongwei Hou [a,*], Yaoting Fan [a]

[a] Department of Chemistry, Zhengzhou University, Zhengzhou 450052, PR China
[b] School of Physical Science and Technology, Suzhou University, Suzhou 215006, PR China

ARTICLE INFO

Article history:
Received 12 March 2008
Received in revised form 6 May 2008
Accepted 9 May 2008
Available online 16 May 2008

Keywords:
Ferrocenylthiocarboxylate
Coordination compounds
Nonlinear optical properties
Electrochemical properties

ABSTRACT

Four metal-organic coordination compounds containing ferrocenylthiocarboxylate components, $[Cd_2(\eta^2\text{-}SOCFc)_2(\eta^1\text{-}\mu_2\text{-}SOCFc)_2(4,4'\text{-bpy})]_n$ (**1**), $[Cd(SOCFc)_2(tmp)]_n$ (tmp = 4,4′-trimethylene-dipyridine) (**2**) $[Zn(SOCFc)_2(2,2'\text{-bpy})]$ (**3**), and $\{[Hg(SOCFc)_2(phen)] \cdot (0.5CH_3OH)\}$ (**4**) (Fc = $(\eta^5\text{-}C_5H_5)Fe(\eta^5\text{-}C_5H_4)$), have been prepared in search of good nonlinear optical (NLO) materials. Investigation of the NLO properties shows that Hg-containing compound **4** exhibits very strong third-order NLO absorptive and refractive effects. The NLO absorptive coefficient α_2 value (2.11×10^{-10} m W^{-1}) is larger than those of all the reported ferrocenylcarboxylate-containing coordination compounds and comparable to the well-performing Hg-containing complexes. Additionally, we further analyzed their NLO behaviors through studying electrochemical properties of the four compounds.

1. Introduction

Over the years, there has been sustained interest in the search of nonlinear optical (NLO) materials due to their potential applications in a wide range such as optical signal processing, all-optical switching, optical computing and other NLO devices [1–3]. These efforts have initially focused on purely inorganic or organic systems [1–4]. Recent interest has been engendered by studying organometallic and coordination compounds [5–8]. Among organometallic compounds, ferrocene derivatives have been the most intensively studied [9–11]. The results show that these compounds possess good NLO properties, it is thought that ferrocenyl conjugated system offers the possibility of electronic communication between terminal subunits, this being of particular interest in nonlinear optics [12]. At the same time, many coordination compounds are found to be good candidates for NLO materials [13], as the incorporation of transition metal ions introduces more sublevels into the energy hierarchy, thus permitting more allowed electronic transitions and giving larger NLO effects [14]. Apparently, ferrocenyl and transition metal ions are responsible for the excellent NLO behavior of their corresponding compounds. Therefore, transition metal coordination compounds containing ferrocenyl may exhibit stronger NLO effects.

Motivated by our interest in nonlinear optical chromophores with ferrocenyl group, in recent years, we have designed and synthesized a series of ferrocene-containing transition metal coordination compounds and studied their NLO behaviors systematically [11,15]. The results suggest that carboxylate-containing ferrocenyl coordination compounds exhibit excellent third-order NLO effects. Considering the similarity between thiocarboxylic acid and carboxylic acid, we believe that some coordination compounds with good NLO properties can be obtained using thiocarboxylate-containing ferrocene derivatives as ligands. Furthermore, compared to the O atom, the S atom possesses much higher electron-donation capability and has empty d orbits which can accept feedback electron from the transition metal ion; this can enhance the extension of the electronic π-system when S atoms coordinate with metal ions. Thus, this type of thiocarboxylate-containing ferrocenyl coordination compounds may have better NLO properties than the corresponding carboxylate-containing ferrocenyl complexes.

Based on the above consideration, in this paper, we selected ferrocenylthiocarboxylic acid (FcCOSH (Fc = $(\eta^5\text{-}C_5H_5)Fe(\eta^5\text{-}C_5H_4)$)) as a ligand and used it to react with the metal salts of Zn(II), Cd(II) or Hg(II) in the existence of some subsidiary ligands. Four coordination compounds, $[Cd_2(\eta^2\text{-}SOCFc)_2(\eta^1\text{-}\mu_2\text{-}SOCFc)_2(4,4'\text{-bpy})]_n$ (**1**), $[Cd(SOCFc)_2(tmp)]_n$ (**2**) $[Zn(SOCFc)_2(2,2'\text{-bpy})]$ (**3**) and $\{[Hg(SOCFc)_2(phen)] \cdot (0.5CH_3OH)\}$ (**4**), were obtained. Investigation of the NLO properties shows that Hg-containing compound **4** possesses very strong third-order NLO absorptive and refractive effects and compounds **1**–**3** exhibit weak third-order NLO behaviors. As far as we known, the NLO absorptive coefficient α_2 value (2.11×10^{-10} m W^{-1}) of **4** is larger than those of all the reported ferrocenylcarboxylate-containing coordination compounds and comparable to the well-performing Hg-containing complexes. In

* Corresponding author. Tel./fax: +86 371 67761744.
E-mail address: houhongw@zzu.edu.cn (H. Hou).

0022-328X/$ - see front matter © 2008 Published by Elsevier B.V.
doi:10.1016/j.jorganchem.2008.05.017

addition, in order to further understand the NLO behaviors of the four coordination compounds, we have studied their electrochemical properties.

2. Experimental

2.1. Materials and physical techniques

The chemicals and solvents used were of A.R. grade and used without further purification. Infrared spectra were recorded on a Bruker Tensor 27 spectrophotometer in the range of 400–4000 cm^{-1} using the KBr pellet technique. UV–Vis spectra were obtained on a HP 8453 spectrophotometer. Elemental analyses of carbon, hydrogen, nitrogen and sulfur were carried out on a FlashEA1112 Elemental Analyzer. NMR spectra were recorded on a Bruker DPX-400 spectrometer.

2.2. Synthesis

2.2.1. Synthesis of ferrocenylthiocarboxylate acid (FcCOSH)

Ferrocenylthiocarboxylic acid (FcCOSH) was prepared according to the literature [16]. Sodium ferrocenylthiocarboxylate (FcCOSNa) was prepared by FcCOSH reacting with CH_3ONa in CH_3OH solution.

2.2.2. Syntheses of compounds **1**–**4**

Synthesis of $[Cd_2(\eta^2\text{-}SOCFc)_2(\eta^1\text{-}\mu_2\text{-}SOCFc)_2(4,4'\text{-bpy})]_n$ (**1**): A methanol solution (4 mL) of 4,4′-bpy (7.8 mg, 0.05 mmol) was added to an aqueous solution (2 mL) of $Cd(OAc)_2 \cdot 2H_2O$ (26.6 mg, 0.1 mmol), and then 6 mL of methanol solution of FcCOSNa (62.4 mg, 0.2 mmol) was added dropwise to the above mixture. The resulting red solution was allowed to stand at room temperature in the dark. Good-quality red crystals were obtained after one week. Yield: 62%. Anal. Calc. for $C_{27}H_{22}CdFe_2NO_2S_2$: C, 47.64; H, 3.26; N, 2.06; S, 9.42. Found: C, 47.58; H, 3.25; N, 2.08; S, 9.39%. IR (cm^{-1}, KBr): 3432(s), 3082(w), 1606(s), 1511(s), 1439(s), 1371(m), 1245(s), 1106(m), 1045(s), 959(m), 823(s), 496(m). ^1H NMR (400 MHz, DMSO-d_6): δ 8.74 (2H, d, J = 5.7 Hz, C_5H_4N), 7.85 (2H, d, J = 5.9 Hz, C_5H_4N), 4.74 (4H, d, J = 1.6 Hz, C_5H_4), 4.41 (4H, s, C_5H_4), 4.21 (10H, s, C_5H_5); ^{13}C NMR (100 MHz, DMSO-d_6): δ 205.7, 150.5, 144.3, 121.3, 83.1, 70.8, 70.2, 70.0.

Synthesis of $[Cd(SOCFc)_2(tmp)]_n$ (**2**): A methanol solution (4 mL) of tmp (19.8 mg, 0.1 mmol) (tmp = 4,4′-trimethylenedipyridine) was added dropwise to an aqueous solution (2 mL) of $Cd(OAc)_2 \cdot 2H_2O$ (26.6 mg, 0.1 mmol), giving a clear solution. FcCOSNa (62.4 mg, 0.2 mmol) in 6 mL of methanol was added dropwise to the above mixture solution. The resulting red solution was allowed to stand at room temperature in the dark. Crystals suitable for X-ray diffraction were obtained three days later. Yield: 73%. Anal. Calc. for $C_{35}H_{32}CdFe_2N_2O_2S_2$: C, 52.49; H, 4.03; N, 3.50; S, 8.01. Found: C, 52.43; H, 4.01; N, 3.51; S, 7.98%. IR(cm^{-1}, KBr): 3428(s), 3085(w), 1610(s), 1555(s), 1435(s), 1371(m), 1243(s), 1103(m), 1047(s), 1018(s), 957(s), 847(s), 607(m), 503(s).^1H NMR (400 MHz, DMSO-d_6): δ 8.47 (4H, d, J = 3.9 Hz, C_5H_4N), 7.27 (4H, d, J = 4.8 Hz, C_5H_4N), 4.74 (4H, t, J = 1.8 Hz, C_5H_4), 4.41 (4H, t, J = 1.8 Hz, C_5H_4), 4.20 (10H, s, C_5H_5), 2.63 (4H, t, J = 7.7 Hz, CH_2), 1.97–1.89 (2H, m, CH_2); ^{13}C NMR (100 MHz, DMSO-d_6): δ 205.6, 150.7, 149.4, 123.9, 83.1, 70.8, 70.2, 70.0, 33.7, 29.9.

Synthesis of $[Zn(SOCFc)_2(2,2'\text{-bpy})]$ (**3**): A methanol solution (6 mL) of FcCOSNa (62.4 mg, 0.2 mmol) was slowly added to a solution of $Zn(OAc)_2 \cdot 2H_2O$ (25.4 mg, 0.1 mmol) and 2,2′-bpy (15.6 mg; 0.1 mmol) in 6 mL of methanol. The resulting red solution was allowed to stand at room temperature in the dark. Crystals of X-ray quality were obtained five days later. Yield: 66%. Anal. Calc. for $C_{32}H_{26}ZnFe_2N_2O_2S_2$: C, 54.00; H, 3.68; N, 3.94; S, 9.01. Found: C, 53.94; H, 3.66; N, 3.96; S, 8.98%. IR(cm^{-1}, KBr): 3427(s), 3080(w), 1606(s), 1586(s), 1474(s), 1441(s), 1370(m), 1315(m), 1240(s), 1106(m), 1041(s), 957(s), 827(s), 767(s), 734(m), 709(m), 503(s). ^1H NMR (400 MHz, DMSO-d_6): δ 8.86–8.72 (4H, m, C_5H_4N), 4.70 (2H, s, C_5H_4), 4.36 (2H, s, C_5H_4), 4.12 (5H, s, C_5H_5); ^{13}C NMR (100 MHz, DMSO-d_6): δ 149.4, 87.9, 70.8, 70.1.

Synthesis of $\{[Hg(SOCFc)_2(phen)] \cdot (0.5CH_3OH)\}$ (**4**): FcCOSNa (62.4 mg, 0.2 mmol) in 6 mL of methanol was added dropwise to a solution of $Hg(OAc)_2$ (31.8 mg, 0.1 mmol) and phen (20 mg, 0.1 mmol) in 6 mL of methanol. After the resulting mixture stood in the dark for two weeks, red crystals of **4** suitable for X-ray diffraction were formed in 52% yield. Anal. Calc. for $C_{34.50}H_{28}Fe_2HgN_2O_{2.50}S_2$: C, 46.72; H, 3.18; N, 3.16; S, 7.23. Found: C, 46.65; H, 3.16; N, 3.18; S, 7.19%. IR(cm^{-1}, KBr): 3430(s), 3080(w), 1611(s), 1509(s), 1432(s), 1369(m), 1237(s), 1103(m), 1041(s), 949(s), 821(s), 729(m), 501(s).^1H NMR (400 MHz, DMSO-d_6): δ 9.18–9.17 (1H, m, CH in phen), 8.63–8.61 (1H, m, CH in phen), 8.08 (1H, s, CH in phen), 7.94–7.91 (1H, m, CH in phen), 4.75 (2H, t, J = 1.9 Hz, C_5H_4), 4.50 (2H, t, J = 1.9 Hz, C_5H_4), 4.19 (5H, s, C_5H_5); ^{13}C NMR (100 MHz, DMSO-d_6): δ 197.6, 150.3, 144.2, 137.4, 129.1, 127.1, 124.1, 81.8, 71.8, 71.1, 70.5, 70.2.

2.3. Crystal structure analysis

All the data were collected on a Rigaku RAXIS-IV imaging plate area detector diffractometer using graphite monochromatic Mo Kα radiation (λ = 0.71073 Å). A prismatic single crystal was mounted on a glass fiber. The data were collected at a temperature of 18 ± 1 °C and corrected for Lorenz-polarization effects. A correction for secondary extinction was applied. The structures were solved by direct methods and expanded using Fourier techniques [17]. The non-hydrogen atoms were refined anisotropically. Hydrogen atoms were included but not refined. The final cycle of full-matrix least-squares refinement was based on observed reflections and variable parameters. All calculations were performed using the SHELXL-97 program [18]. Crystallographic parameters and structural refinement for **1**–**4** are summarized in Table 1. Selected bond lengths and angles are listed in Table 2.

2.4. Nonlinear optical measurements

The DMF solution of compounds **1**–**4** were placed in the 1 mm quartz cuvette, respectively, for NLO measurements. The nonlinear refraction was measured with a linearly polarized laser light (λ = 532 nm; pulse widths = 4.5 ns) generated from a Q-switched and frequency-doubled Nd-YAG laser. The spatial profiles of the optical pulses were nearly Gaussian. The laser beam was focused with a 25-cm focal-length focusing mirror. The radius of the beam waist was measured to be 35 ± 5 μm (half-with at $1/e^2$ maximum). The interval between the laser pulses was chosen to be ~5 s for operational convenience. The incident and transmitted pulse energies were measured simultaneously by two Laser Precision detectors (RjP-735 energy probes), which were linked to a computer by an IEEE interface. The NLO properties of the samples were manifested by moving the samples along the axis of the incident beam (Z-direction) with respect to the focal point [19]. An aperture of 0.5 mm in radius was placed in front of the detector to assist the measurement of the self-focusing effect.

2.5. Differential pulse voltammetry measurements

Differential pulse voltammetry studies were recorded with a CHI660B electrochemical analyzer utilizing the three-electrode configuration, composed of a Pt working electrode, a Pt auxiliary electrode, and a saturated calomel electrode as the reference electrode with a pure N_2 gas inlet and outlet. The measurements were performed in DMF containing tetrabutyl ammonium perchlorate (n-Bu_4NClO_4) (0.1 mol dm^{-3}) as supporting electrolyte, which has

Table 1
Crystal data and structure refinement for compounds **1**–**4**

	1	**2**	**3**	**4**
Formula	$C_{27}H_{22}CdFe_2NO_2S_2$	$C_{35}H_{32}CdFe_2N_2O_2S_2$	$C_{32}H_{26}Fe_2N_2O_2S_2Zn$	$C_{34.50}H_{28}Fe_2HgN_2O_{2.50}S_2$
Formula weight	680.68	800.85	711.74	887.00
Crystal system	Triclinic	Orthorhombic	Monoclinic	Monoclinic
Crystal size (mm)	0.20 × 0.17 × 0.15	0.20 × 0.18 × 0.16	0.20 × 0.17 × 0.16	0.20 × 0.18 × 0.17
Space group	$P\bar{1}$	$P2(1)2(1)2$	$P2(1)/c$	$C2/c$
a (Å)	7.5971(15)	12.220(2)	11.711(2)	21.436(4)
b (Å)	12.149(2)	12.723(3)	10.964(2)	11.009(2)
c (Å)	14.206(3)	10.670(2)	22.985(5)	27.375(6)
α (°)	69.11(3)	90	90	90
β (°)	86.42(3)	90	102.35(3)	97.38(3)
γ (°)	85.62(3)	90	90	90
V (Å^3)	1220.6(4)	1658.9(6)	2883.1(10)	6407(2)
D_c (Mg m^{-3})	1.852	1.603	1.640	1.839
Z	2	2	4	8
μ (mm^{-1})	2.234	1.658	1.997	5.841
Reflection collected/unique [$R_{(int)}$]	3582/3582 [0.0000]	6286/3513 [0.0299]	7201/4356 [0.0531]	8744/5135 [0.0417]
Data/restraints/parameters	3582/0/317	3513/0/108	4356/0/370	5135/1/403
Index ranges	$-9 \leqslant h \leqslant 8$, $-14 \leqslant k \leqslant 0$, $-16 \leqslant l \leqslant 15$	$-15 \leqslant l \leqslant 15$, $-15 \leqslant h \leqslant 0$, $-13 \leqslant l \leqslant 13$	$0 \leqslant h \leqslant 13$, $-12 \leqslant l \leqslant 12$, $-27 \leqslant l \leqslant 26$	$-11 \leqslant h \leqslant 25$, $-13 \leqslant l \leqslant 11$, $-32 \leqslant l \leqslant 32$
F(000)	678	808	1448	3464
Final R_1,[a] wR_2[b]	0.0448, 0.0897	0.0478, 0.1095	0.0540, 0.0763	0.0384, 0.0548
Goodness-of-fit (GOF) on F^2	1.056	1.100	1.032	1.034
$\Delta\rho_{min}$ and $\Delta\rho_{max}$ (e Å^{-3})	0.444 and −0.647	0.612 and −0.581	0.326 and −0.270	0.687 and −0.551

[a] $R_1 = ||F_o| - |F_c||/|F_o|$.
[b] $wR_2 = [w(|F_o^2| - |F_c^2|)^2/w|F_o^2|^2]^{1/2}$. $w = 1/[\sigma^2(F_o)^2 + 0.0297P^2 + 27.5680P]$, where $P = (F_o^2 + 2F_c^2)/3$.

a 50 ms pulse width and a 20 ms sample width. The potential was scanned from +0.4 to +1.0 V at a scan rate of 20 mV s^{-1}.

3. Results and discussion

3.1. Description of crystal structures

Crystallographic analysis reveals that $[Cd_2(\eta^2\text{-SOCFc})_2(\eta^1\text{-}\mu_2\text{-SOCFc})_2(4,4'\text{-bpy})]_n$ (**1**) is a one-dimensional chain polymer composed of alternating binuclear $Cd_2(SOCFc)_4$ units and bridging 4,4′-bpy ligands. A perspective view of the repeating unit, $[Cd_2(SOCFc)_4(4,4'\text{-bpy})]$, and a segment of the polymer are shown in Fig. 1. The $FcCOS^-$ anion has two kinds of coordination modes: chelating bidentate (η^2-SOCFc) and bridging monodentate (η^1–μ_2-SOCFc) modes. In the binuclear unit, each Cd(II) is chelated by a $FcCOS^-$ anion and further, two sulfur atoms from two $FcCOS^-$ anions bridge the two Cd(II) ions in *anti* configuration. These binuclear units are connected by 4,4′-bpy ligands to produce a zigzag chain. Selected bond distances and angles are provided in Table 2. The structure of **1** is similar to that of the reported complex $[\{Cd(SC\{O\}Ph)_2\}_2(\mu\text{-bpy})n]$ [20]. Differently, in $[\{Cd(SC\{O\}Ph)_2\}_2(\mu\text{-bpy})n]$, the carbonyl oxygen atoms of each bridging ligand are also bonded to each Cd(II) metal center.

Table 2
Selected bond lengths (Å) and Angles (deg) for compounds **1**–**4**

Compound **1**			
Cd(1)–N(1)	2.287(5)	Cd(1)–S(2)	2.4498(18)
Cd(1)–O(2)	2.523(4)	Cd(1)–S(1)	2.7904(19)
Cd(1)–S(1)#1	2.5156(18)	S(1)–Cd(1)#1	2.5156(18)
N(1)–Cd(1)–S(2)	98.28(13)	N(1)–Cd(1)–S(1)#1	137.59(12)
Cd(1)#1–S(1)–Cd(1)	88.69(5)	S(2)–Cd(1)–O(2)	62.36(10)
N(1)–Cd(1)–O(2)	82.83(17)	N(1)–Cd(1)–S(1)	89.10(14)
S(1)#1–Cd(1)–S(1)	91.31(5)	O(2)–Cd(1)–S(1)	165.38(10)
S(2)–Cd(1)–S(1)#1	121.87(6)	S(1)#1–Cd(1)–O(2)	102.87(11)
S(2)–Cd(1)–S(1)	107.12(6)		
Compound **2**			
Cd(1)–N(1)#1	2.351(4)	Cd(1)–N(1)	2.351(4)
Cd(1)–S(1)#1	2.5185(16)	Cd(1)–S(1)	2.5185(16)
N(1)#1–Cd(1)–N(1)	94.1(2)	N(1)#1–Cd(1)–S(1)	100.93(16)
N(1)–Cd(1)–S(1)#1	100.93(16)	N(1)#1–Cd(1)–S(1)#1	98.88(15)
N(1)–Cd(1)–S(1)	98.88(15)	S(1)–Cd(1)–S(1)#1	150.77(9)
Compound **3**			
Zn(1)–N(2)	2.075(4)	Zn(1)–N(1)	2.111(4)
Zn(1)–S(1)	2.3262(15)	Zn(1)–S(2)	2.2972(17)
N(2)–Zn(1)–N(1)	78.78(15)	N(1)–Zn(1)–S(2)	107.12(12)
N(2)–Zn(1)–S(2)	118.91(12)	N(2)–Zn(1)–S(1)	124.24(12)
N(1)–Zn(1)–S(1)	111.55(11)	S(2)–Zn(1)–S(1)	109.97(6)
Compound **4**			
Hg(1)–S(2)	2.3723(17)	Hg(1)–S(1)	2.3788(16)
Hg(1)–N(2)	2.589(5)	Hg(1)–N(1)	2.548(4)
S(2)–Hg(1)–S(1)	158.93(6)	S(2)–Hg(1)–N(1)	101.08(11)
S(2)–Hg(1)–N(2)	97.42(11)	S(1)–Hg(1)–N(2)	98.50(11)
S(1)–Hg(1)–N(1)	98.15(10)	N(1)–Hg(1)–N(2)	64.81(14)

Symmetry transformations used to generate equivalent atoms: For **1**: #1 $-x+1, -y, -z+1$; #2 $-x, -y+1, -z+1$. For **2**: #1 $-x+1, -y+2, z$; #2 $-x+1, -y+1, z$.

Compound $[Cd(SOCFc)_2(tmp)]_n$ (**2**) also exhibits a one-dimensional chain structure (Fig. 2), but the structure is not the same as that of **1**. $FcCOS^-$ anions in **2** just exist as monodentate ligands coordinating with Cd(II) ions. The center Cd(II) ion exhibits tetrahedral geometry and coordinates with two terminal S atoms from two $FcCOS^-$ anions and two N atoms from two tmp ligands (Fig. 2). The Cd(II) ion is inside the tetrahedron formed by four coordinated atoms N1–S1–N1A–S1A. The bond distances of Cd–S and Cd–N (2.5185(16) and 2.351(4) Å) are longer than the corresponding bond length of the known polymer $\{[Zn(FcCOO)_2(bpt)] \cdot 2.5H_2O\}_n$ [15c]. The tmp units connect all Cd(II) ions leading to an infinite –Cd–tmp–Cd–tmp– zigzag chain, and the adjacent Cd···Cd distance is 12.723 Å, which is slightly shorter than the Zn···Zn distance (13.619 Å) of the reported polymer $\{[Zn(FcCOO)_2(bpt)] \cdot 2.5H_2O\}_n$.

Compound $[Zn(SOCFc)_2(2,2'\text{-bpy})]$ (**3**) exhibits a mononuclear structure. The Zn(II) ion is in a distorted tetrahedral environment coordinating with two S atoms from two $FcCOS^-$ anions and two N atoms from one 2,2′-bpy ligand. A perspective view of **3** is illustrated in Fig. 3 and selective bond lengths and angles are displayed in Table 2. The Zn–S and Zn–N distances range from 2.075(4) to 2.3262(15) Å and the bond angles around Zn1 vary from 78.78(15) to 124.24(12)°. These $[Zn(SOCFc)_2(2,2'\text{-bpy})]$ units are parallel to each other along the *b*-axis. The shortest centroid-centroid distance between the pyridine rings in 2,2′-bpy ligands of

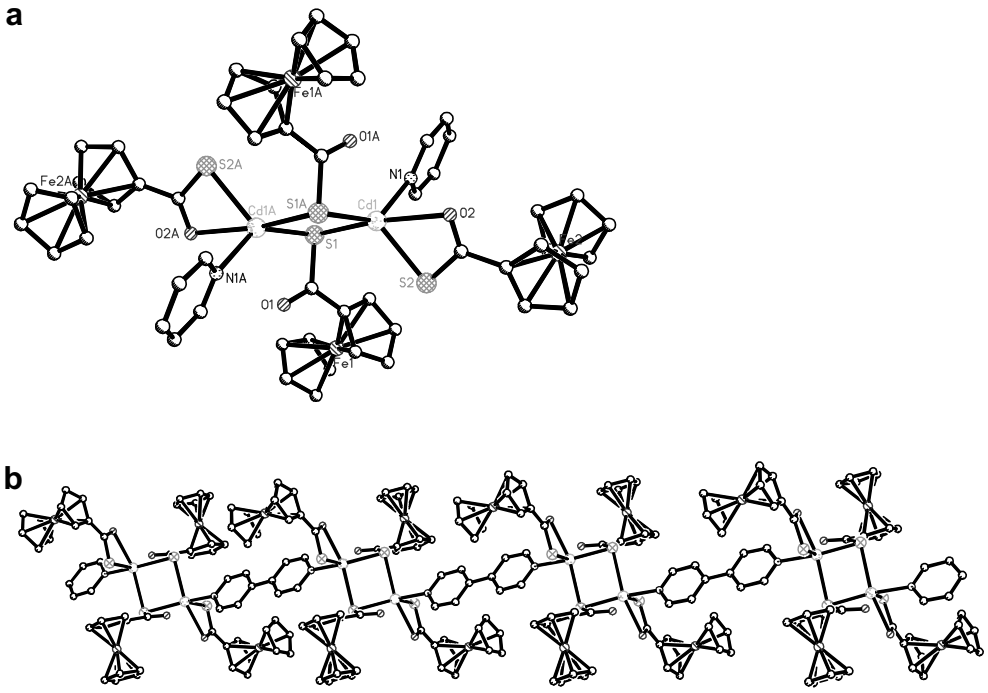

Fig. 1. (a) Perspective view of the repeating unit in $[Cd_2(\eta^2\text{-SOCFc})_2(\eta^1\text{-}\mu_2\text{-SOCFc})_2(4,4'\text{-bpy})]_n$ (**1**). (Hydrogen atoms are omitted for clarity.) (b) A segment of the 1-D polymer **1**.

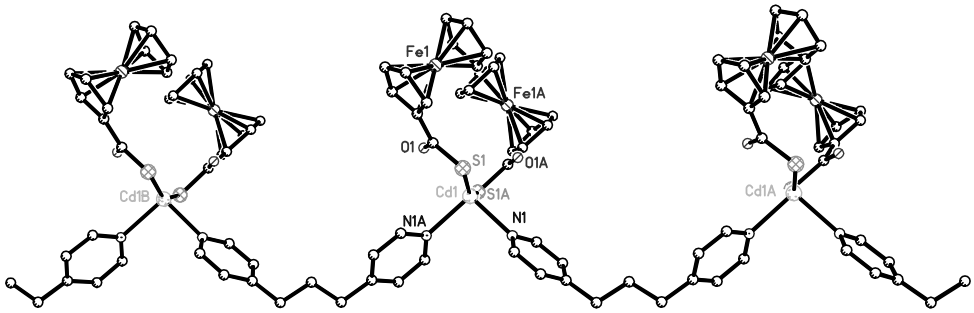

Fig. 2. ORTEP drawing with atom-labeling scheme of the one-dimensional chain polymer $[Cd(SOCFc)_2(tmp)]_n$ (**2**). (Hydrogen atoms are omitted for clarity.)

adjacent units is 4.840 Å, and the displacement angle is 48.1°, so the plane–plane distance is 3.60 Å, indicating the presence of π–π stacking interaction, which is important to stabilize the solid-state structure of compound **3** [21].

X-ray diffraction experiments show that compounds {[Hg(SOCFc)$_2$(phen)] · (0.5CH$_3$OH)} (**4**) and **3** are isomorphous. Similar to **3**, each Hg(II) ion in **4** is bonded to two nitrogen atoms from one chelate phen ligand and two S atoms from two terminal coordinated $FcCOS^-$ anions, furnishing distorted tetrahedral geometry. A perspective view of **4** is illustrated in Fig. 4 and selective bond lengths and angles are displayed in Table 2. The Hg–S and Hg–N distances range from 2.3723(17) to 2.589(5) Å and the bond angles around Hg1 vary from 64.81(14) to 158.93(6)°. The phen rings are coplanar, and they are parallel to each other along the *c*-axis. The shortest distance between two parallel phen rings of adjacent units is 4.389 Å, which is out of the limit of the common range for π–π interactions between two aryl rings [21]. Thus, no obvious intermolecular π–π interactions are found between these phen rings in contrast to compound **3**.

3.2. Nonlinear optical properties

The UV–Vis absorption spectra of compounds **1**–**4** were determined in DMF (Fig. 5). All these compounds have relatively low

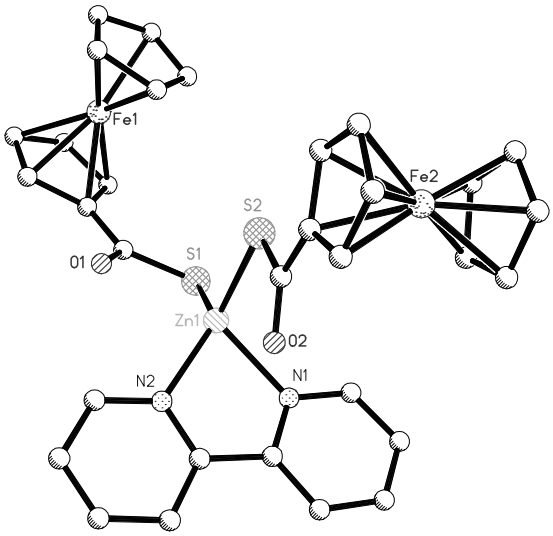

Fig. 3. ORTEP drawing with atom-labeling scheme of $[Zn(SOCFc)_2(2,2'\text{-bpy})]$ (**3**). (Hydrogen atoms are omitted for clarity.)

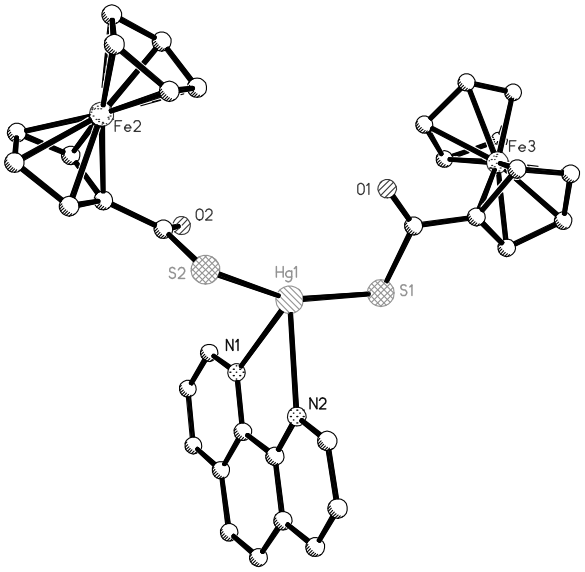

Fig. 4. ORTEP drawing with atom-labeling scheme of {[Hg(SOCFc)$_2$-(phen)] · (0.5CH_3OH)} (**4**). (Hydrogen atoms and solvent molecule are omitted for clarity.)

linear absorption ranging from 500 to 800 nm, promising low-intensity loss and little temperature change caused by photon absorption when light propagates in the materials. This demonstrates that the NLO responses are clear without interference of other absorption at λ = 532 nm used in the *Z*-scan technique.

The NLO properties of **1**–**4** were investigated with laser pulse of wavelength 532 nm and duration 4.5 ns by a *Z*-scan experiment in DMF solution [19,22]. We found that compound **4** possesses large NLO absorption and strong refractive effects, and compounds **1**–**3** exhibit weak third-order NLO absorptive and refractive effects. The NLO absorption components were evaluated by a *Z*-scan experiment using an open-aperture configuration. The NLO refractive effects are assessed by dividing the normalized *Z*-scan data obtained under the closed aperture configuration by the normalized *Z*-scan data obtained under the open aperture configuration.

Fig. 6a depicts the NLO absorptive properties of compound **4** in a DMF solution. A reasonably good fit between the experimental data (filled squares) and the theoretical curve (solid curve) suggests that the experimentally obtained NLO effects are effectively third-order in nature. The figure clearly illustrates that the absorption increases as the incident light irradiance rises since light transmittance (*T*) is a function of the sample's *Z* position. It can be seen from Fig. 6a that

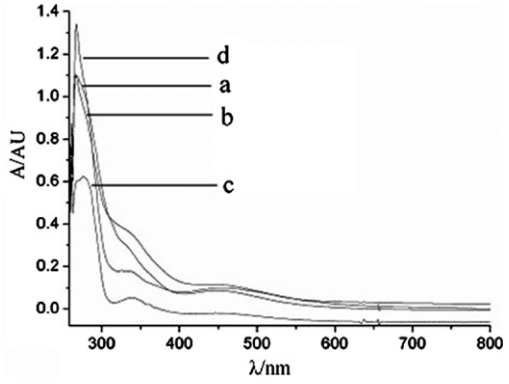

Fig. 5. The UV–Vis spectra of (a) **1**, (b) **2**, (c) **3** and (d) **4** in DMF.

the normalized transmittance drops to about 28% at the focus; the corresponding third-order NLO absorptive coefficient α_2 is calculated to be 2.11×10^{-10} m W^{-1}. To the best of our knowledge, the value is larger than those of all the reported ferrocenylcarboxylate-containing coordination compounds [11] and comparable to the well-performing Hg-containing complexes such as $[HgI_2(4,4'\text{-azopyridine})]_n$ ($\alpha_2 = 1.3 \times 10^{-11}$ m W^{-1}) [23a], $[HgI_2(bpea)]_n$ ($\alpha_2 = 1.1 \times 10^{-11}$ m W^{-1}) [23b] and $[Hg_2(dcapp)_2]$ (weak) [23c] etc.

Fig. 6b depicts the NLO refractive effects of compound **4**. The valley and peak occur at equal distances from the focus. The result is consistent with the notion that observed optical nonlinearity has an effective third-order dependence on the incident electromagnetic field [19]. A reasonably good fit between the experimental data (black squares) and the theoretical curves (solid curves) was obtained. The effective third-order nonlinear refractive index n_2 value is calculated to be 1.61×10^{-17} m^2 W^{-1} by the equation $n_2 = [\lambda\alpha_0/0.812\pi I(1 - e^{\alpha_0 L})]\ \Delta T_{v\text{-}p}$. Obviously, the value is better than those of the reported Hg complexes such as $[HgI_2(L)]$ (L = 1,2-bis[(ferrocen-l-ylmethylene)amino]ethane) ($n_2 = 8.02 \times 10^{-19}$ m^2 W^{-1}) [24a], $[Hg(bpfb)I_2]_n$·2DMF ($n_2 = 6.854 \times 10^{-18}$ m^2 W^{-1}) [24b] and $[Hg_2(dcapp)_2]$ ($n_2 = 3.653 \times 10^{-18}$ m^2 W^{-1}) [23c] etc.

As mentioned above, compound **4** possesses stronger third-order NLO property than some reported coordination compounds. Compared with the O atom, the S atom possesses much higher electron-donation capability and has empty d orbits which can accept feedback electron from the transition metal ion, and the π-electron delocalization of the molecular is extending with the forming of the compound, then the α_2 and n_2 values of **4** are larger than those of ferrocenylcarboxylate-containing coordination compounds. In addition, all the four compounds contain FcCOSH and similar subsidiary ligands, but only **4** exhibits strong non-linear absorptive and refractive performance. We presume that metal ions make an important contribution to the NLO properties. It can be further explained by the heavy-atom effect: the strength of the NLO properties can be altered by the π-back-donation capacity of the metal ions to the ligands, and the increased π-back-donation capacity of the metal ions to the ligands may enhance the extension of the electronic π system and improve the NLO properties [14]. For example, in the reported polymers $[Co(bbbt)_2(NCS)_2]_n$ ($n_2 = 5.73 \times 10^{-19}$ m^2 W^{-1}), $[Mn(bbbt)_2(NCS)_2]_n$ ($n_2 = 3.55 \times 10^{-19}$ m^2 W^{-1}) and $[Cd(bbbt)_2(NCS)_2]_n$ ($n_2 = 3.07 \times 10^{-19}$ m^2 W^{-1}), $[Co(bbbt)_2(NCS)_2]_n$ possesses the strongest NLO properties just because the electronic π back-donation capacity of Co^{2+} is the largest among the three kinds of ions [15a]. Therefore, due to the higher π back-donation capacity of Hg(II) compared to Zn(II) and Cd(II), Hg-containing compound **4** gives stronger NLO effects than compounds **1**–**3**. This phenomenon is also observed in other reported complexes such as Pb(II) and Zn(II) compounds [15b], Cd(II) and Zn(II) complexes [25a], as well as Cr, Mo and W compounds [25b]. In a word, the combination of the soft S donor (with the higher electron-donation capability) and the soft Hg acceptor (with the higher back-donation capability) has greatly enhanced the extension of the electronic π-system, so compound **4** possesses very strong third-order NLO property.

3.3. Electrochemistry

Generally, there is a certain relationship between the optical and electrochemical properties. To further understand the NLO behavior of the four compounds, we studied their electrochemical properties.

The solution-state differential pulse voltammetry for FcCOSNa and **1**–**4** shows single peaks with half-wave potentials at 0.664, 0.788, 0.764, 0.776 and 0.696 V (versus SCE), respectively (Fig. 7). These observed redox peaks correspond to the single-electron Fe(II)/Fe(III) couple oxidation process. Compared with that of the

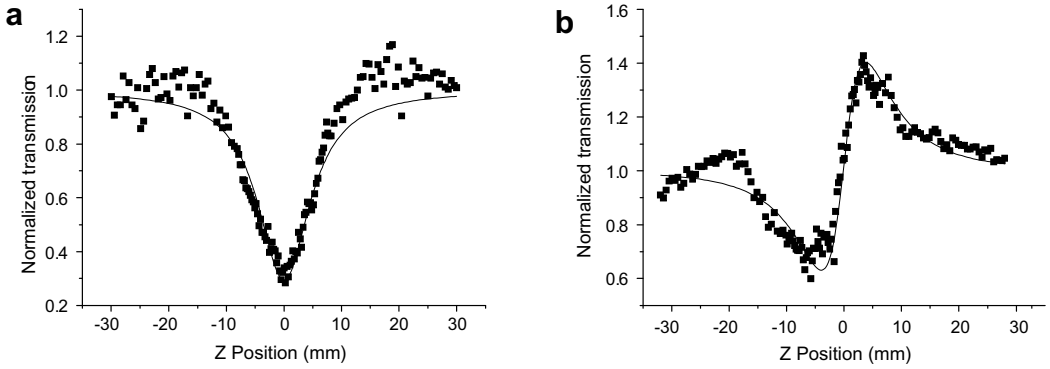

Fig. 6. *Z*-scan data for **4** in DMF solution, (a) obtained under an open aperture configuration, (b) obtained by dividing the normalized *Z*-scan measured under a closed aperture configuration by the normalized *Z*-scan data obtained under the open aperture configuration. The black dots are the experimental data, and the solid curve is the theoretical fit.

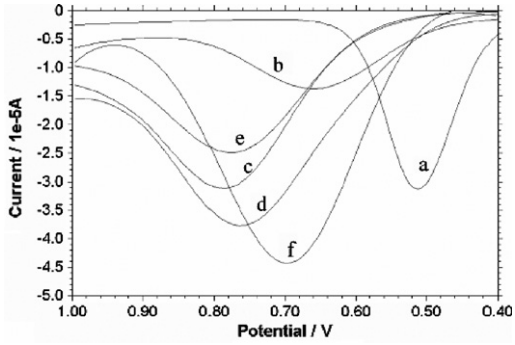

Fig. 7. Differential pulse voltammogram of (a) ferrocene, (b) FcCOSNa, (c) **1**, (d) **2**, (e) **3** and (f) **4** (1.0×10^{-3} M) in DMF containing *n*-Bu_4NClO_4 (0.1 M) at a scan rate of 20 mV s^{-1} (vs. SCE).

free ferrocene (0.512 V), the half-wave potential of the free ligand (FcCOSNa) is shifted to higher potential. Obviously, the electron-withdrawing group (–COS^-) makes the Fe(II) centers harder to oxidize. At the same time, the potentials of **1**–**4** are higher than that of the free ligand. This is due to the presence of conjugated π-electron systems between the Fe(II) center and the coordinated metal ion in the four compounds, which permits electronic communication between the two metal centers. Consequently, as found with other ferrocenyl-containing coordination compounds [15d,26], the electron-withdrawing nature of the coordinated metal center makes the ferrocene unit harder to oxidize.

In addition, the half-wave potential of **4** occurs at a lower value when compared to other three compounds, indicating that Fe(II) centers in **4** are more easily oxidized to Fe(III). This, in turn, shows that electron cloud density around Fe(II) in **4** is quite bigger than that of other three compounds, which could be further attributed to the higher back-donation capability of Hg(II) compared to Zn(II) and Cd(II). Therefore, through electrochemical studies, we further demonstrated the existence of the electronic communication and the delocalization of the π-electron cloud between the iron centers and coordinated metal centers. Moreover, the extent of the delocalization for **4** is greater. And then, it is reasonable that compound **4** exhibits very strong NLO properties.

In recent years, we have been seeking the factors that affect the NLO properties of coordination compounds, and have synthesized series of compounds with excellent NLO properties according to our research. We believe that our exploration may provide a useful guide to the design of good third-order NLO materials.

Acknowledgements

This work was financially supported by the National Natural Science Foundation (No. 20671082), NCET and the Ph.D. Programs Foundation of Ministry of Education of China.

Appendix A. Supplementary material

Supplementary data associated with this article can be found, in the online version, at doi:10.1016/j.jorganchem.2008.05.017.

References

[1] (a) J. Zyss (Ed.), Molecular Nonlinear Optics, Academic Press, New York, 1994;
(b) N.P. Prasad, D.J. Williams, Introduction to Nonlinear Optical Effects in Molecules and Polymers, Wiley, New York, 1991.
[2] (a) J.A. McCleverty, T.J. Meyer, Nonlinear optical properties of metal complexes, in: B.J. Coe (Ed.), Comprehensive Coordination Chemistry, vol. 2, Elsevier, Pergamon, 2004 (Chapter 9.14);
(b) H.S. Nalwa, S. Miyata (Eds.), Nonlinear Optics of Organic Molecules and Polymers, CRC Press, Boca Raton, FL, 1997;
(c) Z.Y. Tian, W.T. Huang, D.B. Xiao, S.Q. Wang, Y.S. Wu, Q.H. Gong, W.S. Yang, J.N. Yao, Chem. Phys. Lett. 391 (2004) 283.
[3] (a) L.R. Dalton, A.W. Harper, R. Ghosn, W.H. Steier, M. Ziari, H. Fetterman, Y. Shi, R.V. Mustacich, A.K.Y. Jen, K.J. Shea, Chem. Mater. 7 (1995) 1060;
(b) D.M. Burland, Chem. Rev. 94 (1994) 1.
[4] (a) P.R. Varanasi, A.K.Y. Jen, J. Chandrasekhar, I.N.N. Namboothiri, A. Rathna, J. Am. Chem. Soc. 118 (1996);
(b) M. Blanchard-Desce, V. Alain, P.V. Bedworth, S.R. Marder, A. Fort, C. Runser, M. Barzoukas, S. Lebus, R. Wortmann, Chem. Eur. J. 3 (1997) 1091;
(c) G.G.A. Balavoine, J.-C. Daran, G. Iftime, P.G. Lacroix, E. Manoury, Organometallics 18 (1999) 21.
[5] (a) N.J. Long, Angew. Chem., Int. Ed. Engl. 34 (1995) 21;
(b) I.R. Whittall, A.M. McDonagh, M.G. Humphrey, Adv. Organomet. Chem. 42 (1998) 291;
(c) A.M. McDonagh, M.G. Humphrey, M. Samoc, B. Luther-Davies, Organometallics 18 (1999) 5195.
[6] (a) B.J. Coe, T.A. Hamor, C.J. Jones, J.A. McCleverty, D. Bloor, G.H. Cross, T.L. Axon, J. Chem. Soc., Dalton Trans. (1995) 673;
(b) D.R. Kanis, P.G. Lacroix, M.A. Ratner, T.J. Marks, J. Am. Chem. Soc. 116 (1994) 10089.
[7] (a) M.E. Wright, E.G. Toplikar, H.S. Lackritz, J.T. Kerney, Macromolecules 27 (1994) 3016;
(b) G.C. Yang, Z.M. Su, C.S. Qin, J. Phys. Chem. A 110 (2006) 4817.
[8] (a) D. Roberto, R. Ugo, F. Tessore, E. Lucenti, Organometallics 21 (2002) 161;
(b) L. Wang, M. Yang, G.H. Li, Z. Shi, S.H. Feng, Inorg. Chem. 45 (2006) 2474;
(c) Y.Q. Wei, Y.F. Yu, K.C. Wu, Cryst. Growth Des. 7 (2007) 2262;
(d) K. Liang, H.G. Zheng, Y.L. Song, Y.Z. Li, X.Q. Xin, Cryst. Growth Des. 7 (2007) 373;
(e) R. Bronisz, Inorg. Chem. 46 (2007) 6733;
(f) Z.G. Ren, H.X. Li, G.F. Liu, W.H. Zhang, J.P. Lang, Y. Zhang, Y.L. Song, Organometallics 25 (2006) 4351;

(g) J. Wang, Z.R. Sun, L. Deng, Z.H. Wei, W.H. Zhang, Y. Zhang, J.P. Lang, Inorg. Chem. 46 (2007) 11381;
(h) W.H. Zhang, Y.L. Song, Y. Zhang, J.P. Lang, Cryst. Growth Des. 8 (2008) 253.
[9] (a) P. Nguyen, P. Gómez-Elipe, I. Manners, Chem. Rev. 99 (1999) 1515;
(b) K.N. Jayaprakash, P.C. Ray, I. Matsuoka, M.M. Bhadbhade, V.G. Puranik, P.K. Das, H. Nishihara, A. Sarkar, Organometallics 18 (1999) 3851;
(c) I.S. Lee, H. Seo, Y.K. Chung, Organometallics 18 (1999) 1091.
[10] (a) Y.H. Liu, Y.L. Lu, H.C. Wu, J.C. Wang, K.L. Lu, Inorg. Chem. 41 (2002) 2592;
(b) G. Baskar, K. Landfester, M. Antonietti, Macromolecules 33 (2000) 9228;
(c) R.C. Squire, S.M.J. Aubin, K. Folting, W.E. Streib, D.N. Hendrickson, G. Christou, Angew. Chem., Int. Ed. Engl. 34 (1995) 887.
[11] G. Li, Y.L. Song, H.W. Hou, L.K. Li, Y.T. Fan, Y. Zhu, X.R. Meng, L.W. Mi, Inorg. Chem. 42 (2003) 913.
[12] J.A. Mata, E. Peris, S. Uriel, R. Llusar, I. Asselberghs, A. Persoons, Polyhedron 20 (2001) 2083.
[13] (a) O.R. Evans, H.L. Ngo, W. Lin, J. Am. Chem. Soc. 123 (2001) 10395;
(b) W.B. Lin, Z.Y. Wang, L. Ma, J. Am. Chem. Soc. 121 (1999) 11249.
[14] H. Chao, R.H. Li, B.H. Ye, H. Li, X.L. Feng, J.W. Cai, J.Y. Zhou, L.N. Ji, J. Chem. Soc., Dalton Trans. (1999) 3711.
[15] (a) H.W. Hou, X.R. Meng, Y.L. Song, Y.T. Fan, Y. Zhu, H.J. Lu, C.X. Du, W.H. Shao, Inorg. Chem. 41 (2002) 4068;
(b) X.R. Meng, Y.L. Song, H.W. Hou, Y.T. Fan, G. Li, Y. Zhu, Inorg. Chem. 42 (2003) 1306;
(c) H.W. Hou, L.K. Li, G. Li, Y.T. Fan, Y. Zhu, Inorg. Chem. 42 (2003) 3501;
(d) J. Wu, Y.L. Song, E.P. Zhang, H.W. Hou, Y.T. Fan, Y. Zhu, Chem. Eur. J. 12 (2006) 5823.
[16] T. Katada, M. Nishida, S. Kato, M. Mizuta, J. Organomet. Chem. 129 (1977) 189.
[17] G.M. Sheldrick, Acta Crystallogr. A 46 (1990) 467.
[18] G.M. Sheldrick, SHELXL-97, Program for the Refinement of Crystal Structures, University of Göttingen, 1997.
[19] M. Sheik-Bahae, A.A. Said, T.H. Wei, D.J. Hagan, E.W. Van Stryland, IEEE J. Quantum Electron. 26 (1990) 760.
[20] J.J. Vittal, J.T. Sampanthar, Z. Lu, Inorg. Chim. Acta 343 (2003) 224.
[21] (a) D. Guo, K.L. Pang, C.Y. Duan, C. He, Q.J. Meng, Inorg. Chem. 41 (2002) 5978;
(b) C. Janiak, J. Chem. Soc., Dalton Trans. (2000) 3885.
[22] H.W. Hou, X.Q. Xin, J. Liu, M.Q. Chen, S. Shi, J. Chem. Soc., Dalton Trans. (1994) 3211.
[23] (a) Y.Y. Niu, Y.L. Song, T.N. Chen, Z.L. Xue, X.Q. Xin, CrystEngCommun 36 (2001) 1;
(b) Y.Y. Niu, Y.L. Song, H.W. Hou, H.G. Zheng, X.Q. Xin, Chin. J. Inorg. Chem. 17 (2001) 723;
(c) H.W. Hou, Y.L. Wei, Y.L. Song, L.W. Mi, M.S. Tang, L.K. Li, Y.T. Fan, Angew. Chem., Int. Ed. Engl. 44 (2005) 2.
[24] (a) H.W. Hou, G. Li, Y.L. Song, Y.T. Fan, Y. Zhu, L. Zhu, Eur. J. Inorg. Chem. 12 (2003) 2325;
(b) Y.Y. Niu, Y.L. Song, J. Wu, H.W. Hou, Y. Zhu, X. Wang, Inorg. Chem. Commun. 7 (2004) 471.
[25] (a) Y.T. Fan, D.X. Xue, G. Li, H.W. Hou, C.X. Du, H.J. Lu, J. Mol. Struct. 707 (2004) 153;
(b) J. Mata, S. Uriel, E. Peris, R. Llusar, S. Houbrechts, A. Persoons, J. Organomet. Chem. 562 (1998) 197.
[26] (a) S.S. Sun, J.A. Anspach, A.J. Lees, Inorg. Chem. 41 (2002) 1862;
(b) T. Morikita, T. Yamamoto, J. Organomet. Chem. 637 (2001) 809;
(c) R. Horikoshi, T. Mochida, H. Moriyama, Inorg. Chem. 41 (2002) 3017.